# Dispersion relations for Bernstein waves in a relativistic pair plasma

Ramandeep Gill[*] and Jeremy S. Heyl[†]

*Department of Physics and Astronomy, University of British Columbia, 6224 Agricultural Road, Vancouver,*
*British Columbia, Canada V6T 1Z1*

A fully relativistic treatment of Bernstein waves in an electron-positron pair plasma has remained too formidable a task, owing to the very complex nature of the problem. In this paper, we perform contour integration of the dielectric-response function and numerically compute the dispersion curves for a uniform magnetized relativistic electron-positron pair plasma. The behavior of the dispersion solution for several cases with different plasma temperatures is highlighted. In particular, we find two wave modes that exist only for large wavelengths and frequencies similar to the cyclotron frequency in a moderately relativistic pair plasma. The results presented here have important implications for the study of those objects where a hot magnetized electron-positron plasma plays a fundamental role in generating the observed radiation.

## I. INTRODUCTION

Relativistic electron-positron pair plasmas are found in many astrophysical objects such as neutron star magnetospheres [1], relativistic jets, and accretion disks associated with black holes in the centers of active galactic nuclei [2,3]. To study the properties of the pair plasma in these objects it is imperative to employ a fully relativistic approach. In the study of magnetized pair plasmas one finds that a number of oscillation modes exist (see [4,5]). The focus of this study is to investigate the behavior of Bernstein modes in a uniform magnetized relativistic $e^+e^-$ pair plasma. Bernstein waves are electrostatic undulations that are always localized near the electron cyclotron harmonics in an electron-ion plasma [6]. These waves can propagate undamped only very close to the plane perpendicular to the static magnetic field. Such waves are of great interest since, in an electron-ion plasma, they strongly interact with the electrons and are excellent candidates for plasma heating and driving currents as compared with the electromagnetic (O)rdinary and the e(X)traordinary modes [7].

The nonrelativistic treatment of Bernstein waves in an electron-ion plasma is well understood [8–11]. It is the fully relativistic case that is marred by difficulties such that a closed-form analytic solution is hard to formulate or maybe even impossible. Many workers have expounded on the fully relativistic treatment of electron Bernstein waves [12], the ultrarelativistic case [13], and have successfully obtained approximate dispersion relations [14–16]. The Bernstein mode in a weakly relativistic pair plasma has been investigated by the authors of [17], where they have found closed curve dispersion relations that are remarkably distinct from the classical case. All of these studies either discuss the fully relativistic case to the point where no closed-form analytic solution is found, or simplify the analysis by either treating the limiting case only or employ various approximations that may not yield an entirely correct result.

In this paper, we present a fully relativistic treatment of Bernstein waves in a pair plasma and provide dispersion curves that highlight the transition from the weakly to strongly relativistic regime. The rest of the article is organized as the following. We derive the key equations for the dielectric-response tensor and describe our numerical approach to the problem in the following section (Sec. II). In Sec. III, we present the main results of this study along with a discussion on how the solution behaves as a function of the plasma temperature and plasma frequency. In the final section (Sec. IV) we highlight some of the important points of the study.

## II. RELATIVISTIC DISPERSION RELATION

The evolution of the distribution function, $f(\mathbf{r},\mathbf{p},t)$, of plasma particles in phase space is governed by the Vlasov equation, which in the momentum representation is given as

$$\frac{\partial f_s}{\partial t} + \mathbf{v} \cdot \nabla_\mathbf{r} f_s + q_s(\mathbf{E} + \mathbf{v} \times \mathbf{B}) \cdot \nabla_\mathbf{p} f_s = 0, \tag{1}$$

where $s$ indicates different species constituting the plasma. To investigate the behavior of small amplitude waves with oscillation periods much smaller than particle collision times, we make the following assumptions:

$$f_s(\mathbf{r},\mathbf{p},t) = f_{0s}(p) + f_{1s}(\mathbf{r},\mathbf{p},t), \tag{2}$$

$$\mathbf{B} = \mathbf{B_0} + \mathbf{B}_1 e^{i(\mathbf{k}\cdot\mathbf{r}-\omega t)}, \tag{3}$$

$$\mathbf{E} = \mathbf{E}_1 e^{i(\mathbf{k}\cdot\mathbf{r}-\omega t)}, \tag{4}$$

where the subscripts 0 and 1 indicate equilibrium and perturbed functions, respectively. Furthermore, we restrict the equilibrium distribution function to only depend on the momentum of the particles to account for the anisotropy introduced by the ambient static magnetic field. As a result, we write the Vlasov equation in its linearized form

*rsgill@phas.ubc.ca
†Corresponding author; heyl@phas.ubc.ca

$$\frac{d}{dt}f_{1s} = -q_s(\mathbf{E}_1 + \mathbf{v} \times \mathbf{B}_1)e^{i(\mathbf{k} \cdot \mathbf{r} - \omega t)} \cdot \nabla_{\mathbf{p}}f_{0s}. \tag{5}$$

The main idea here is to calculate the perturbation of the distribution function by integrating along the unperturbed orbits from some time in the past, say $t_0$, to the present time $t$. Next, we use Ohm's law to write the current density induced by the perturbed distribution

$$\mathbf{J} = \sum_s \frac{q_s}{m_s} \int \mathbf{p}_s f_{1s}(\mathbf{r}, \mathbf{p}, t) d^3 p = \sum_s \underline{\underline{\sigma}}_s \cdot \mathbf{E_1}. \tag{6}$$

This enables us to write the effective dielectric permittivity tensor in terms of the conductivity tensor $\underline{\underline{\sigma}}$ [8],

$$\underline{\underline{\epsilon}}(\omega, \mathbf{k}) = \epsilon_0 \left( I - \frac{\underline{\underline{\sigma}}}{i\omega_s \epsilon_0} \right). \tag{7}$$

In the fully relativistic approximation, the energy and linear momentum of particles in the rest frame of the plasma are given as

$$\mathcal{E} = \gamma mc^2 = \sqrt{p^2 c^2 + m^2 c^4},$$

$$\mathbf{p} = \gamma m\mathbf{v}, \tag{8}$$

where the Lorentz factor is given in terms of the momentum as

$$\gamma = \left( 1 + \frac{p^2}{m^2 c^2} \right)^{1/2}. \tag{9}$$

The complete details of the rest of the calculation can be found in various monographs and textbooks on plasma waves (see [8,10]), and we only provide the salient points of the derivation in what follows. We adopt $\mathbf{B}_0 = B_0 \hat{z}$ for the equilibrium magnetic field and restrict both the wave vector and the perturbed electric field to be $\mathbf{k} = k_\perp \hat{x}$ and $\mathbf{E}_1 = E_1 \hat{x}$ as dictated by the purely electrostatic mode, where the perturbed magnetic field $\mathbf{B}_1$ vanishes. After some mathematical manipulations we arrive at the relativistic dielectric tensor,

$$\underline{\underline{\epsilon}}(\omega, \mathbf{k}) = \begin{pmatrix} \epsilon_{xx} & \epsilon_{xy} & 0 \\ -\epsilon_{xy} & \epsilon_{yy} & 0 \\ 0 & 0 & \epsilon_{zz} \end{pmatrix}, \tag{10}$$

where the different components have been summed over both species, $e^+$ and $e^-$, of the pair plasma,

$$\epsilon_{xx} = \epsilon_0 \Bigg[ 1 + \frac{4\pi q^2 m^2}{k_\perp^2 m\epsilon_0} \int \left\{ \frac{\pi \gamma a}{\sin \pi \gamma a} J_{\gamma a}(\xi) J_{-\gamma a}(\xi) \right.$$
$$\left. - 1 \right\} \frac{\gamma}{p_\perp} \frac{\partial f_0(p)}{\partial p_\perp} p^2 \sin \theta dp d\theta \Bigg],$$

$$\epsilon_{yy} = \epsilon_0 \Bigg[ 1 + \frac{4\pi q^2}{\omega m\epsilon_0} \int \frac{p_\perp}{\omega_c} \frac{\partial f_0(p)}{\partial p_\perp} \left\{ \frac{\pi}{\sin \pi \gamma a} \times J'_{\gamma a}(\xi) J'_{-\gamma a}(\xi) \right.$$
$$\left. + \frac{a}{\gamma \xi^2} \right\} p^2 \sin \theta dp d\theta \Bigg],$$

$$\epsilon_{zz} = \epsilon_0 \Bigg[ 1 + \frac{4\pi q^2}{\omega m\epsilon_0 \omega_c} \int p_\parallel \frac{\partial f_0(p)}{\partial p_\parallel}$$
$$\times \frac{\pi J_{\gamma a}(\xi) J_{-\gamma a}(\xi)}{\sin \pi \gamma a} p^2 \sin \theta dp d\theta \Bigg],$$

$$\epsilon_{xy} = i \frac{4\pi q^2 m^2}{m k_\perp^2} \int \frac{\gamma}{p_\perp} \frac{\partial f_0(p)}{\partial p_\perp} p^2 \sin \theta dp d\theta. \tag{11}$$

In the above, $\parallel$ and $\perp$ subscripts denote components parallel and perpendicular to the equilibrium magnetic field, $J_{\gamma a}(\xi)$ is the Bessel function of noninteger order, and $J'_{\gamma a}(\xi)$ is the derivative of the Bessel function with respect to $\xi$, where $\xi = \frac{k_\perp p_\perp}{qB}$, and $a = \frac{\omega}{\omega_c}$ with $\omega_c$ denoting the nonrelativistic cyclotron frequency. Finally, one finds the dispersion relation, $\omega = \omega(\mathbf{k})$, by setting the dielectric-response function to zero,

$$\epsilon(\omega, \mathbf{k}) = \mathbf{k} \cdot \underline{\underline{\epsilon}}(\omega, \mathbf{k}) \cdot \mathbf{k} = 0, \tag{12}$$

which in our case simply picks out the $\epsilon_{xx}$ component. To keep the treatment fully relativistic we adopt the Maxwell-Boltzmann-Jütner distribution function [8,18],

$$f_0(p) = (4\pi m^3 c^3)^{-1} \frac{\eta}{K_2(\eta)} e^{-\eta\gamma}, \tag{13}$$

where

$$\eta \equiv \frac{mc^2}{k_B T} \tag{14}$$

is the ratio of the rest mass energy of the particles to that of their thermal energy, and $K_2$ is the modified Bessel function of the second kind and of order two. Also, the equilibrium plasma distribution has been normalized to unity,

$$1 = n_0 = \int f_0(p) d^3 p. \tag{15}$$

Taking the derivative of $f_0(p)$ with respect to $p_\perp$ and $p_\parallel$ yields

$$\frac{\partial f_0}{\partial p_i} = -\frac{\eta^2}{4\pi m^5 c^5 K_2(\eta)} \frac{p_i}{\gamma} e^{-\eta\gamma}, \tag{16}$$

where $i$ can be replaced by either $\parallel$ or $\perp$ components. At this point, we can carry out the integration over the polar angle and by defining $\beta = \frac{k_\perp p}{qB}$ we can write $\epsilon_{xx}$ as the following:

$$\epsilon_{xx} = \epsilon_0 \Bigg[ 1 - \frac{\omega_p^2 \eta^2}{k_\perp^2 m^3 c^5 K_2(\eta)} \int_0^\infty p^2 e^{-\eta\gamma}$$
$$\times \int_0^\pi \left\{ \frac{\pi \gamma a}{\sin \pi \gamma a} J_{\gamma a}(\beta \sin \theta) J_{-\gamma a}(\beta \sin \theta) \right.$$
$$\left. - 1 \right\} \sin \theta d\theta dp \Bigg], \tag{17}$$

where the nonrelativistic plasma frequency is defined as

$$\omega_p^2 = \frac{n_0 e^2}{m \epsilon_0}. \qquad (18)$$

Next we use the following Bessel function identity [8]:

$$\int_0^\pi \sin \theta J_a(b \sin \theta) J_{-a}(b \sin \theta) d\theta$$

$$= \frac{2 \sin \pi a}{\pi a} {}_2F_3\left(\frac{1}{2}, 1; \frac{3}{2}, 1-a, 1+a; -b^2\right) \qquad (19)$$

to express the integral over the polar angle in terms of a hypergeometric function, and redefine all constants and variables to make $\epsilon_{xx}$ dimensionless,

$$\hat{p} = \frac{p}{mc} \quad \hat{k}_\perp = \frac{k_\perp c}{\omega_c} \quad \hat{\omega} = \frac{\omega}{\omega_c},$$

$$\hat{\omega}_p = \frac{\omega_p}{\omega_c} \quad \beta = \hat{\beta} = \hat{k}_\perp \hat{p} \quad a = \hat{\omega}. \qquad (20)$$

Then, we can write $\epsilon_{xx}$ as the following where the integral now is just over the dimensionless momentum $\hat{p}$:

$$\epsilon_{xx} = \epsilon_0 \left[ 1 - \frac{2\hat{\omega}_p^2 \eta}{\hat{k}_\perp^2} \left\{ \frac{\eta}{K_2(\eta)} \int_0^\infty \hat{p}^2 e^{-\eta\gamma} \right. \right.$$

$$\left. \left. \times {}_2F_3\left(\frac{1}{2}, 1; \frac{3}{2}, 1-\gamma\hat{\omega}, 1+\gamma\hat{\omega}; -\hat{\beta}^2\right) d\hat{p} - 1 \right\} \right].$$
$$(21)$$

In writing this equation we have made use of the following integral identity:

$$\int_0^\infty \hat{p}^2 e^{-\eta\gamma} d\hat{p} = \frac{K_2(\eta)}{\eta}. \qquad (22)$$

The integrand in Eq. (21) consists of a hypergeometric function which is singular for $1 - \gamma\hat{\omega} = -n$ for integer $n = 0, 1, 2, \ldots,$. This singular behavior, as we shall see, is associated to the phenomenon of cyclotron resonance where plasma particles are in resonance with the wave at the cyclotron harmonics. Also, this very resonance poses a real challenge for any numerical computation of the integral and has to be dealt with using advanced numerical techniques. Since our interest lies in finding the oscillation frequency $\hat{\omega}$ as a function of the wave number $\hat{k}_\perp$, it is clear from Eq. (21) that this operation is explicitly nonlinear. Therefore, one is left with an exercise of root finding for a given $\hat{\omega}$. Alternatively, one could simplify the analysis by making some approximation. However, by adopting such methodology one risks losing the subtleties of the solution and may obtain something that is not entirely correct, as we show in the weakly relativistic case. We remain optimistic and decide to compute the dispersion relation using a brute force method, which is by simply integrating Eq. (21).

### Numerical approach

As the Lorentz factor is a function of momentum, the integrand remains singular over the domain of integration. A
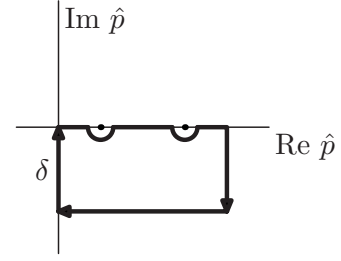


FIG. 1. Contour of integration in the complex $\hat{p}$ plane used to avoid singular points of the integrand. Only the general case is shown here to guide the reader.

workaround for avoiding the singular points on the real axis is by analytically continuing the momentum to the complex domain. We can easily shift the integration contour below the real axis by writing $p \rightarrow p - i\delta$, where $\delta$ is reasonably small. Ideally, one would like to keep the contour on the real axis but go below the singular points to avoid divergence while following the Landau prescription [19]. A similar result can be achieved by closing the contour of integration in the lower half of the complex plane as shown in Fig. 1.

Here we are interested in finding the principal value of the integral in Eq. (21), which is given by the following:

$$\text{P.V.} \int_0^\infty d\hat{p} f(\hat{p}) = i\pi \sum_{\text{Residue}} R_0 - (I_2 + I_3 + I_4), \qquad (23)$$

where

$$I_2 = \int_\infty^{\infty - i\delta} d\hat{p} f(\hat{p}) \approx 0,$$

$$I_3 = \int_{\infty - i\delta}^{-i\delta} d\hat{p} f(\hat{p}),$$

$$I_4 = \int_{-i\delta}^0 d\hat{p} f(\hat{p}), \qquad (24)$$

and $R_0$ is the residue from the poles on the $\text{Re}(\hat{p})$ axis. In the above, for $I_2$ we note that the integrand vanishes sufficiently rapidly for large $\hat{p}$ due to the exponential. When $\hat{\omega}$ and $\hat{k}_\perp$ are kept real, one finds that $R_0$ is also real, which makes the first term on the right in Eq. (23) purely imaginary. However, the second term has both real and imaginary components, and the negative sign is indicative of the clockwise sense of the contour. Since the left-hand side is real then so must be the right, which suggests that the imaginary components cancel each other and yields the following result:

$$\text{P.V.} \int_0^\infty d\hat{p} f(\hat{p}) = -\text{Re}(I_3 + I_4). \qquad (25)$$

Although it appears that with the given prescription one can have an arbitrarily large $\delta$, we find that the integral does start to lose its accuracy as $\delta$ approaches unity. Therefore, we set $\delta = 0.1$ for all numerical computations. To compute the integral numerically over the hypergeometric function we
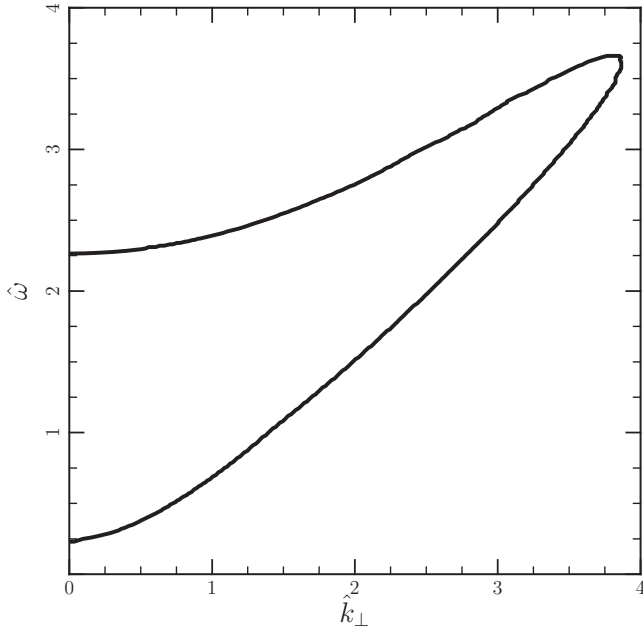
FIG. 2. Dispersion curve for a relativistic plasma with $\eta=1$, $\hat{\omega}_p=3$. Hatted variables are expressed in terms of the nonrelativistic cyclotron frequency $\omega_c$. See text for more detail.

used MATHEMATICA (V.6) for it is capable of calculating generalized hypergeometric functions. The poles of the integrand were dealt with by employing a globally adaptive integration routine available in MATHEMATICA. To speed up the integration over the singular points we used the Double Exponential Quadrature singularity handler built into the integration routine of MATHEMATICA.

## III. PROPERTIES OF DISPERSION CURVES

In the nonrelativistic case of the electron Bernstein modes in an electron-ion plasma, one finds that there are no wave modes below the first harmonic. The dispersion curves above the hybrid frequency are all bell shaped with local maxima corresponding to stationary modes. Furthermore, band gaps are present above the hybrid frequency between each dispersion curve. It is not at all surprising to say that the picture is remarkably different in the relativistic pair plasma scenario. We plot the dispersion curves for a relativistic pair plasma in Figs. 2–4 for different values of $\eta=1,5,20$, respectively. We assume a plasma frequency of $\hat{\omega}_p=3$ for these plots.

The dispersion relation for a moderately relativistic pair plasma, shown in Fig. 2, clearly has two wave modes. This is further accompanied by the existence of two stationary modes with vanishing group velocity ($d\hat{\omega}/d\hat{k}_\perp=0$) at two distinct oscillation frequencies for $\hat{k}_\perp=0$. Also, above the higher stationary mode there are two wave-number solutions for a given $\hat{\omega}$. This behavior persists in the case of a mildly relativistic pair plasma, shown in Fig. 3. However, one sees some drastic changes in the shape of the dispersion curves as the particles lose their energy. We readily notice the appearance of the curve near the cyclotron fundamental frequency. This marks the onset of the cyclotron resonance where the

plasma particles oscillate at the same frequency as the perturbing electrostatic wave. Although not very significant at this point, the higher harmonic resonances also start to emerge. Furthermore, the dispersion relation now extends to higher wave numbers and the turnover from the lower wave mode into the upper mode is not as sharp as it was in the previous case. We also notice a shift in the stationary modes, and we discuss this point in a later section.

The authors of [17] reported the dispersion relation for a weakly relativistic pair plasma. They found island shaped
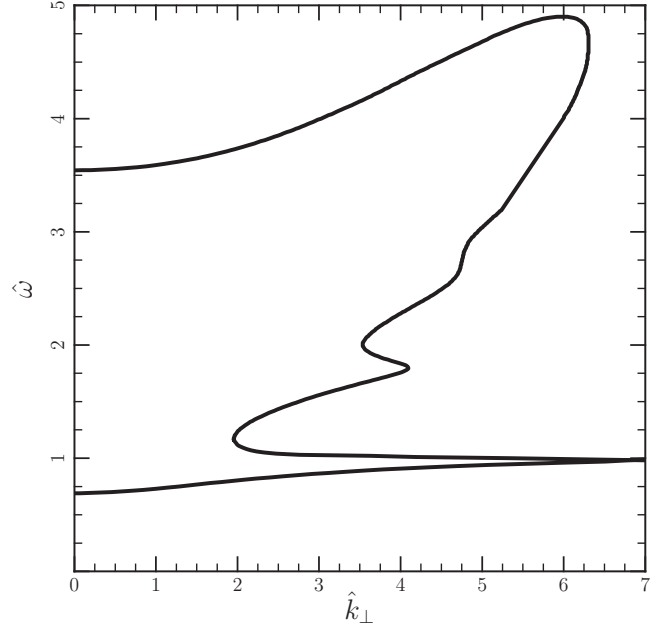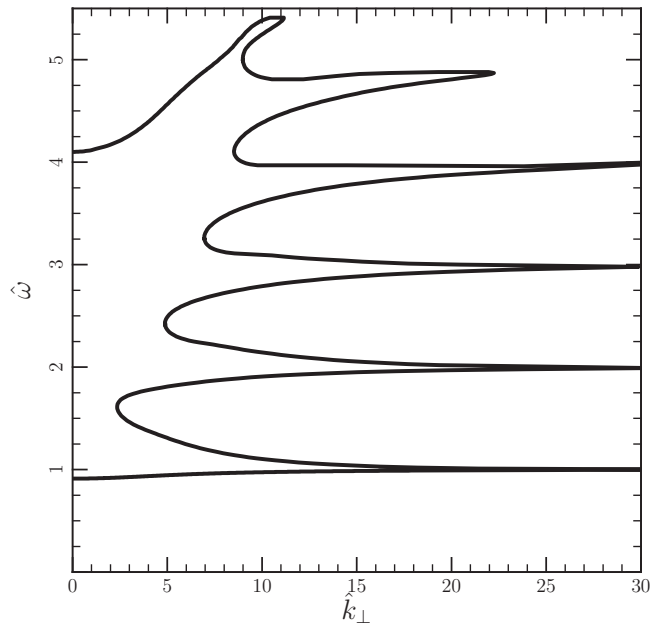


FIG. 3. Dispersion curve for a relativistic plasma with $\eta=5$, $\hat{\omega}_p=3$. Hatted variables are expressed in terms of the nonrelativistic cyclotron frequency $\omega_c$. See text for more detail.



FIG. 4. Dispersion curve for a relativistic plasma with $\eta=20$, $\hat{\omega}_p=3$. Hatted variables are expressed in terms of the nonrelativistic cyclotron frequency $\omega_c$. See text for more detail.

curves occurring mostly between the cyclotron harmonics. We find a similar solution for the weakly relativistic case, shown in Fig. 4, but with a few exceptions. First, the dispersion curves are no longer closed but extend to higher wave numbers as they approach cyclotron harmonics. This behavior is very similar to what we observe in the case of a non-relativistic electron-ion plasma. However, in the pair plasma case the solution does not extend to an infinitely large wave number, and there are not infinitely many wave modes as we increase $\hat{\omega}$. There appears to be a cutoff in frequency, the point where the overturn takes place, beyond which there does not exist any solution. Second, there exists a wave mode below the fundamental cyclotron harmonic, which was absent in the solution provided in [17]. In fact, we find that a solution below the cyclotron fundamental exists for all cases, regardless of $\eta$, for $\hat{\omega}_p = 3$ as we show below. This, again, is in contrast with the nonrelativistic electron-ion plasma where there is no wave mode below the first harmonic.

In comparison to the moderately relativistic case, the weakly relativistic case is richer in its behavior as well as much more structured. The former only has two frequency modes for a given wavelength, namely, a high and a low mode, and the latter has many. Moreover, for a moderately relativistic pair plasma none of the wave modes found in between the two stationary points (discussed below) extend to infinitely small wavelengths. In fact, there is a limiting wavelength above which these modes exist. As reported in [17], one can find similar, although much less severe, imperfections in the graphics produced by the contouring algorithm. The culprit here is the nonlinearity of the equation from which the solutions are obtained.

### A. Relativistic effects

As the plasma particles become strongly relativistic, with decreasing $\eta$, the dispersion curves undergo drastic changes. We now plot all of the dispersion curves shown earlier onto a single plot and analyze the progression from the weakly relativistic case to the strongly relativistic one (see Fig. 5). The Bernstein waves are strongly absorbed near the cyclotron harmonics in the weakly relativistic limit, where $\eta \gg 1$. This effect is the strongest at the first cyclotron harmonic at which point the phase velocity of the wave $v_{ph} \to 0$ and the wave loses all of its energy in heating up the pair plasma. At higher harmonics the same phenomenon is repeated, however with decreased efficiency. Upon increasing the thermal speed of the plasma particles, the cyclotron resonances become much less pronounced and start to disappear completely. In a hot magnetized pair plasma no resonant interaction between the Bernstein wave and the plasma occurs, and the solution occupies only a small region of the $\hat{\omega} - \hat{k}_\perp$ space.

### B. Behavior for small $\hat{k}_\perp$

Unlike the nonrelativistic electron Bernstein waves, the behavior of the dispersion curves in the limit of vanishing wave number is not so straightforward. The hypergeometric function in the integrand of Eq. (21) can also be written in the form of an infinite power series [8],
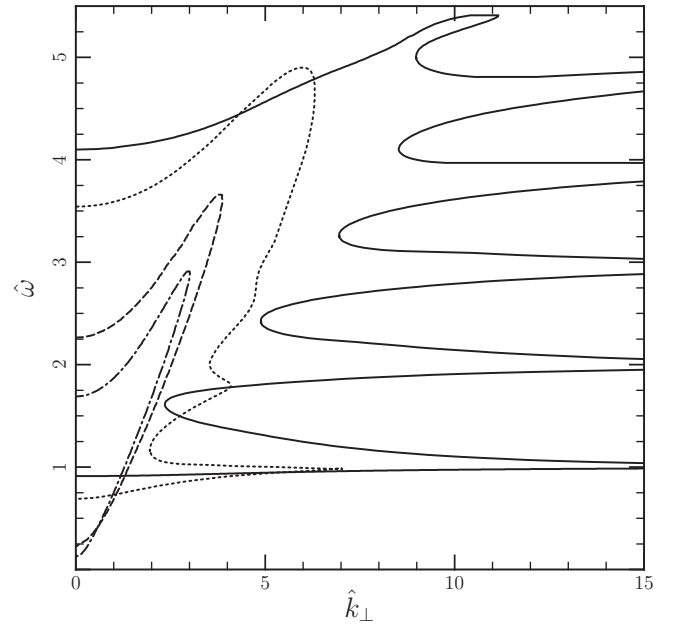


FIG. 5. Dispersion curves for different values of $\eta$ with $\hat{\omega}_p = 3$. (Solid) The weakly relativistic case with $\eta = 20$, (dots) the mildly relativistic case with $\eta = 5$, and the two strongly relativistic cases: (a) (dash) with $\eta = 1$ (b) (dot-dash) with $\eta = 0.5$

$$
\begin{aligned}
{}_2F_3 & (a_1, a_2; b_1, b_2, b_3; x) \\
&= \frac{\Gamma(b_1)\Gamma(b_2)\Gamma(b_3)}{\Gamma(a_1)\Gamma(a_2)} \\
&\quad \times \sum_{m=0}^{\infty} \frac{\Gamma(a_1+m)\Gamma(a_2+m)}{\Gamma(b_1+m)\Gamma(b_2+m)\Gamma(b_3+m)} \frac{x^m}{m!}.
\end{aligned} \quad (26)
$$

We see that for $x \to 0$ only the $m=0$ term has the dominant contribution. In that case, we find that the hypergeometric function tends to unity. Consequently, $\epsilon_{xx}$ loses its dependence on $\hat{\omega}$ because the only place $\hat{\omega}$ appears in Eq. (21) is inside the hypergeometric function. Moreover, this suggests that $\hat{\omega}(\hat{k}_\perp)$ is constant in the domain where $\hat{k}_\perp \ll 1$ and Eq. (21) fails to describe the behavior of the dispersion relation for vanishing $\hat{k}_\perp$. In fact, one has to keep terms in the infinite sum up to order $m=2$ to obtain any nontrivial solution. However, upon doing so one finds that the integral, again, is extremely nontrivial and its solution cannot be expressed analytically. This is problematic because the dispersion solution is no longer a smooth function and may become discontinuous for small $\hat{k}_\perp$.

Nevertheless, this problem can be resolved easily. Upon cursory inspection of the integrand one finds that it is quadratic in $\hat{k}_\perp$, making it symmetric under the transformation $\hat{k}_\perp \to -\hat{k}_\perp$. Furthermore, we demand that the dispersion relation be continuous at $\hat{k}_\perp = 0$; thus, we employ polynomial interpolation to determine the $y$ intercept. In all three figures we use a polynomial of order 2 or 4, depending on the shape of the curve, to determine the stationary points for vanishing wave number.

### C. Behavior for large $\hat{k}_\perp$

In the weakly relativistic case, one finds wave-particle resonances occurring at cyclotron harmonics. These resonances extend to large values of $\hat{k}_\perp$ but not to infinity. Intuitively, one may argue, by looking at the rest of the dispersion solution, that such a behavior is expected as the dispersion curves start and end at $\hat{k}_\perp = 0$. The plot remains connected over the whole domain, as is evident in the strongly relativistic case, and the resonances only extend to some maximum value of the wave number $\hat{k}_\perp^{\text{Max}}$. This hypothesis can be ascertained by computing the integral in Eq. (21) for $\hat{k}_\perp \gg 1$; however for large values of $\hat{k}_\perp$ the calculation becomes very computationally expensive.

Ideally, one would like to find the asymptotic behavior of the hypergeometric function in Eq. (21) to simplify the problem. The asymptotic behavior of the hypergeometric function can be gleaned by asymptotically expanding the Bessel function in the integral representation of the hypergeometric function given in Eq. (20). The Bessel function expansion for large arguments is given as [20]

$$J_{\pm\nu}(z) = \sqrt{\frac{2}{\pi z}} \cos\left(z \mp \frac{\pi}{2}\nu - \frac{\pi}{4}\right) + \mathcal{O}(z^{-3/2}). \quad (27)$$

Plugging this back into Eq. (20) and carrying out the integral over the polar angle yields

$$\frac{2}{\pi b} \int_0^\pi d\theta \cos\left(b \sin\theta - \frac{\pi}{2}a - \frac{\pi}{4}\right) \cos\left(b \sin\theta + \frac{\pi}{2}a - \frac{\pi}{4}\right)$$

$$= \frac{\cos(a\pi) + H_0(2b)}{b}, \quad (28)$$

where $H_0$ is the Struve function of order 0. For our specific case, $b = \hat{k}_\perp \hat{p}$ and $a = \gamma\hat{\omega}$, and upon substitution of this result into the dielectric-response function we find

$$\epsilon_{xx} = \epsilon_0 \left[ 1 - \frac{2\hat{\omega}_p^2 \eta}{\hat{k}_\perp^2} \left\{ \frac{\eta}{2\hat{k}_\perp K_2(\eta)} \int_0^\infty \hat{p} e^{-\eta\gamma} \right. \right.$$

$$\left. \left. \times \left(\frac{\pi\gamma\hat{\omega}}{\sin \pi\gamma\hat{\omega}}\right) [\cos \pi\gamma\hat{\omega} + H_0(2\hat{k}_\perp \hat{p})] d\hat{p} - 1 \right\} \right]. \quad (29)$$

This integral again has a similar singularity for $\gamma\hat{\omega} = n$ for integer $n$. We can further simplify this equation by noting the leading-order behavior of the Struve function in the limit $b \to \infty$, which goes like $H_0(b) \propto \frac{1}{\sqrt{b}}$. Then, in this limit the dominant term in Eq. (29) is the cosine term. Although this step is not justifiable given the limits of integration where the integrand is evaluated for $\hat{p} \ll 1$, this does not modify the overall behavior of the dielectric-response function in the large $\hat{k}_\perp$ limit. Next, we define

$$\mathcal{I}(\eta, \hat{\omega}) = \pi\hat{\omega} \int_0^\infty d\hat{p}\, \gamma\hat{p} e^{-\eta\gamma} \cot(\pi\gamma\hat{\omega}) \quad (30)$$

and solve for $\epsilon_{xx} = 0$. After some rearrangement of terms, we arrive at a cubic equation, which we then solve for $\hat{k}_\perp$,

$$\hat{k}_\perp^3 + 2\hat{\omega}_p^2 \eta \hat{k}_\perp - \frac{\hat{\omega}_p^2 \eta^2}{K_2(\eta)} \mathcal{I}(\eta, \hat{\omega}) = 0. \quad (31)$$

To do the integral in Eq. (30) we again employ the same contour integration scheme as was done earlier (see Fig. 1). For $\eta = 20$ and $\hat{\omega} = 1$, which is the strongest resonance of all occurring at higher cyclotron harmonics, we find a maximum wave number $\hat{k}_\perp^{\text{Max}} \sim 72$. We find values of the same order for resonances at higher harmonics as well. This limit shows the maximum value of $\hat{k}_\perp$ for which a solution exists using the simplified dielectric tensor (appropriate for large values of $\hat{k}_\perp$). The actual limits to the wave number in the realistic dispersion relation are typically lower. This exercise demonstrates that the resonances do not extend to infinitely small wavelengths, that there is some cutoff at $\hat{k}_\perp \sim \hat{k}_\perp^{\text{Max}}$, and that the dispersion curves remain connected over the whole domain. More importantly, one must not forget that this estimate is particularly inaccurate for the strongly relativistic case where the solution exists for only modest values of $\hat{k}_\perp$.

### D. Stationary modes

There are two stationary modes ($v_g = d\hat{\omega}/d\hat{k}_\perp = 0$) present for vanishing $\hat{k}_\perp$ in all the cases shown above. We plot the evolution of both stationary points as a function of $\eta$ in Fig. 6. For $\omega_p = 3\omega_c$ the upper stationary mode remains above the cyclotron fundamental and the lower stationary mode remains below it for all $\eta$. Contrastingly, in the electron-ion case a solution exists for vanishing $\hat{k}_\perp$ at all cyclotron harmonics, except at the fundamental. It appears that the upper stationary mode turns into the hybrid resonance given by

$$\hat{\omega}_H^2 = \hat{\omega}_p^2 + 1 \quad (32)$$

in an electron-ion plasma.

This picture is slightly modified as we lower the plasma frequency so that it equals the cyclotron frequency, $\hat{\omega}_p = 1$, while remaining in the weakly relativistic limit with $\eta = 20$ (see Fig. 7). We still find those two stationary points and the strong resonance at the cyclotron fundamental; however, the rest of the plot has disappeared, and, interestingly, been replaced by a single closed curve. By comparing the present case to the one treated previously, with $\hat{\omega}_p = 3$, we find that upon decreasing the plasma frequency the lower branch of the dispersion curve in the first harmonic band separates from the upper branch. Also the upper branch in the first harmonic band connects to the lower branch in the second-harmonic band. This is the first incidence where a closed curve solution, like the ones found by the authors of [17], has appeared in our analysis. Furthermore, the number of stationary modes is now double of what was observed previously.

We also provide a plot of the position of stationary points in frequency as a function of the plasma frequency for dif-
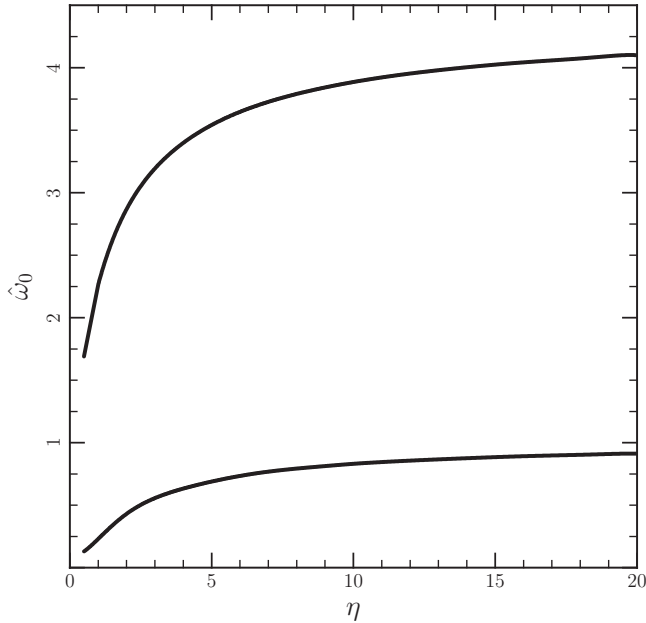
FIG. 6. Stationary modes at vanishing $\hat{k}_\perp$ as a function of non-dimensional reciprocal temperature parameter $\eta$. The upper curve corresponds to the upper stationary mode and the lower curve to the lower stationary mode. For this plot we assume $\hat{\omega}_p = 3$.

ferent values of $\eta = 1, 5, 20$ (see Fig. 8). As the slope of the curves varies with a change in $\eta$, the upper hybrid frequency, if one was to associate the upper stationary mode with it, necessarily depends on the temperature of the plasma, as shown in Fig. 6. Interestingly, in the case of a hot pair plasma ($\eta \lesssim 1$) we find that the upper stationary mode extends below the cyclotron fundamental for $\hat{\omega}_p < 1$. Thus, an underdense ($\omega_p < \omega_c$) strongly relativistic pair plasma does not have any Bernstein wave modes above the cyclotron fun-
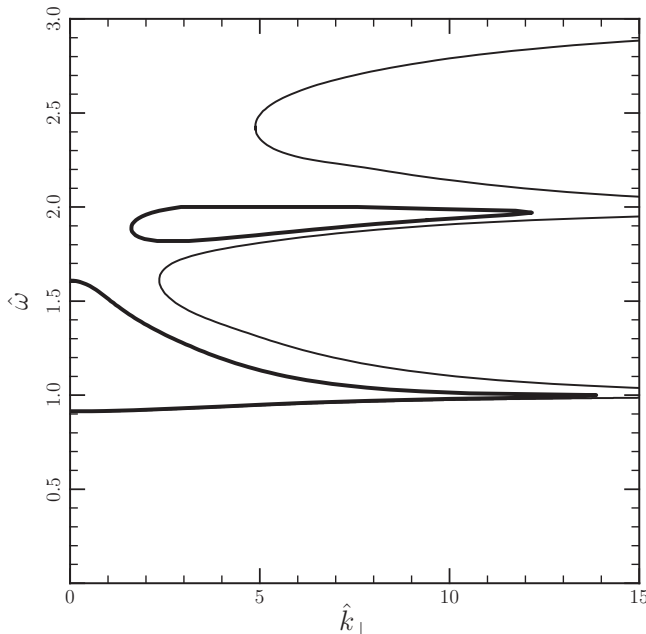


FIG. 7. Dispersion curves at two different plasma frequencies with $\eta = 20$. (a) For $\hat{\omega}_p = 3$, and (b) (bold) for $\hat{\omega}_p = 1$.
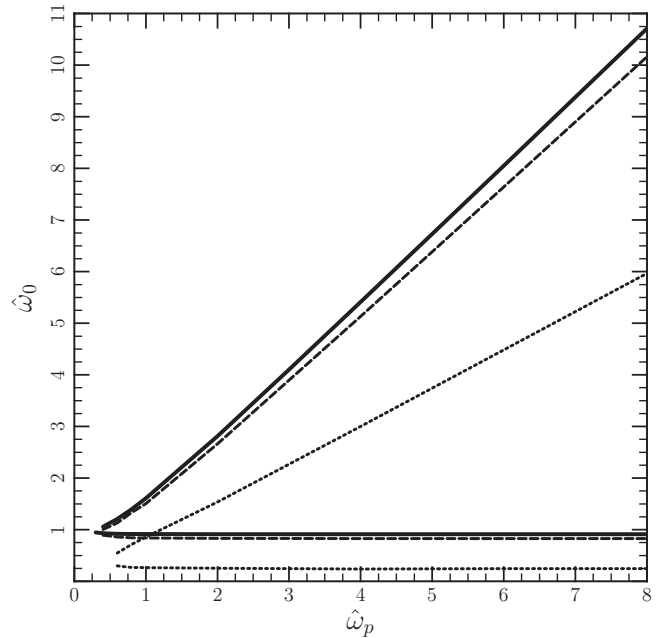


FIG. 8. Stationary modes as a function of the plasma frequency at different values of the reciprocal temperature parameter $\eta$. (a) (Solid) For $\eta = 20$, (b) (dash) for $\eta = 10$, and (c) (dot) for $\eta = 1$.

damental. Another consequence of this situation is that the two wave modes exist for only small wave numbers and therefore for extremely large wavelengths. We see that for a given plasma temperature, the upper stationary mode depends linearly on the plasma frequency for $\hat{\omega}_p > 1$. On the other hand, the lower mode remains constant.

## IV. DISCUSSION

In this article, we investigate the behavior of Bernstein waves in a uniform magnetized relativistic electron-positron pair plasma and provide dispersion curves for different values of the nondimensional reciprocal temperature. The dispersion solutions in all cases are found to be remarkably different than the Bernstein modes found in the nonrelativistic electron-ion case. For a moderately relativistic pair plasma we find two Bernstein wave modes accompanied by two stationary modes for vanishing wave number. We do not find closed curve solutions [17] in all cases but one where the plasma frequency equals the cyclotron frequency in the weakly relativistic limit.

As stated earlier, the Bernstein waves in a nonrelativistic electron-ion plasma propagate undamped in the direction orthogonal to the equilibrium magnetic field. This might not be true for such waves in a relativistic pair plasma. These waves were found to be very weakly damped in a weakly relativistic pair plasma [21]. In this article, we only report the real component of $\hat{\omega}$ as the imaginary component is quite nontrivial to calculate for the following reason. With $\hat{\omega}$ complex Eq. (25) does not hold since the principal value of the integral is no longer purely real. As a result, one must calculate the residue $R_0$, which itself is a difficult task as the integrand in Eq. (21) cannot be easily transformed into the following

form where the singularity arises due to a simple pole of order $m$:

$$f(\hat{p}) = \frac{g(\hat{p})}{(\hat{p} - \hat{p}_0)^m},\tag{33}$$

and where $g(\hat{p})$ is analytic as $\hat{p} \to \hat{p}_0$. Nevertheless, we do expect very mild damping of the waves ($\hat{\omega}_i \ll \hat{\omega}_r$) at least for the weakly relativistic case as discussed in [21], where they find $\mathrm{Im}(\hat{\omega})$ to be the largest on the upper half of the curve that advances toward the cyclotron harmonics, and relatively much smaller on the lower half. It remains to be seen if damping is at all observed in the moderately relativistic case.

The results presented in this article have important implications for all astronomical objects where a magnetized hot pair plasma is present, for example radio pulsars [1], magnetars [22], and pair-instability supernovae [23].

[1] M. A. Ruderman and P. G. Sutherland, Astrophys. J. **196**, 51 (1975).

[2] M. C. Begelman, R. D. Blandford, and M. J. Rees, Rev. Mod. Phys. **56**, 255 (1984).

[3] F. Takahara and M. Kusunose, Prog. Theor. Phys. **73**, 1390 (1985).

[4] D. B. Melrose, Plasma Phys. Controlled Fusion **39**, A93 (1997).

[5] M. Gedalin, D. B. Melrose, and E. Gruman, Phys. Rev. E **57**, 3399 (1998).

[6] I. B. Bernstein, Phys. Rev. **109**, 10 (1958).

[7] J. Decker and A. K. Ram, Phys. Plasmas **13**, 112503 (2006).

[8] D. G. Swanson, *Plasma Waves*, 2nd ed., IOP Conf. Proc. (Institute of Physics, London, 2003).

[9] N. A. Krall and A. W. Trivelpiece, *Principles of Plasma Physics*, 1st ed. (McGraw-Hill, New York, 1973).

[10] W. Baumjohann and R. A. Treumann, *Basic Space Plasma Physics*, 1st ed. (Imperial College Press, London, 1996).

[11] J. P. Dougherty, Phil. Trans. Soc. London A **280**, 95 (1975).

[12] A. Georgiou, Plasma Phys. Controlled Fusion **38**, 347 (1996).

[13] B. Buti, Phys. Fluids **6**, 89 (1963).

[14] A. N. Saveliev, Plasma Phys. Controlled Fusion **47**, 2003 (2005).

[15] A. N. Saveliev, Plasma Phys. Controlled Fusion **49**, 1061 (2007).

[16] F. Volpe, Phys. Plasmas **14**, 122105 (2007).

[17] D. A. Keston, E. W. Laing, and D. A. Diver, Phys. Rev. E **67**, 036403 (2003).

[18] R. Schlickeiser, Phys. Scr. **T75**, 33 (1998).

[19] L. D. Landau, J. Phys. (Moscow) **10**, 25 (1946).

[20] I. S. Gradshteyn and I. M. Ryzhik, *Table of Integrals, Series, and Products*, 7th ed. (Academic Press, New York, 2007).

[21] E. W. Laing and D. A. Diver, Phys. Rev. E **72**, 036409 (2005).

[22] C. Thompson and R. C. Duncan, Mon. Not. R. Astron. Soc. **275**, 255 (1995).

[23] C. L. Fryer, S. E. Woosley, and A. Heger, Ap. J. **550**, 372 (2001).